Title
A MULTIPERIPHERAL MODEL OF MESON AND BARYON MULTIPLICITIES

Author
Koplik, Joel.

Publication Date
1972-12-01

Submitted to Physical Review D

LBL-1539
Preprint c.1

A MULTIPERIPHERAL MODEL OF MESON AND BARYON MULTIPLICITIES

Joel Koplik

December 14, 1972

Prepared for the U.S. Atomic Energy Commission under Contract W-7405-ENG-48

A MULTIPERIPHERAL MODEL OF MESON AND BARYON MULTIPLICITIES*

Joel Koplik

Lawrence Berkeley Laboratory
University of California
Berkeley, California 94720

December 14, 1972

ABSTRACT

We construct a simple coupled-channel multiperipheral model of mesons and baryons in order to calculate their respective multiplicities at high energy. By requiring total cross sections to have their usual Regge behavior the baryon multiplicity is necessarily small, with an upper bound not far from the experimental value. More precise results are difficult to obtain in this context. Arguments are given that this result will be valid in more realistic models.

I. INTRODUCTION

One striking feature of the recent ISR data is the small magnitude and steep rise with energy of the multiplicity of baryons with respect to mesons (see Fig. 1 and Refs. 1 and 9). The increase with energy can be understood intuitively in terms of the large ratio of masses: the multiplicity is expected to become appreciable only when the energy is high enough to produce many particles, and much more energy is needed to create baryons--especially via $B\bar{B}$ pairs--than pions. In the framework of multiperipheral models one can be more specific and say that the limiting $\log s$ behavior of the average multiplicity will occur only when $\log s$ is large enough for many partial cross sections to contribute, and at a given energy more of these are accessible to lower mass particles. In this paper we will be more concerned with the small limiting[2] ratio, which may also be anticipated in this context for two reasons. First, it is a characteristic of multiperipheral models that the average rapidity interval between clusters of produced particles increases with the mass of the cluster. In the ABFST model[3] for example, it is found[4] that the average interval, w, in $\log s$ between links in the multiperipheral chain is roughly given by

$$\cosh w \approx 1 + s_0/2|t_{max}| \qquad (1)$$

where $(s_0)^{\frac{1}{2}}$ is the mass emitted at each link and $|t_{max}|$ is the effective upper limit of momentum transfer. (This property is most easily seen in the simplified model discussed by Chan and Webber;[5] we will say more about this in Sec. II.) Since baryons are likely to be emitted from more massive clusters than mesons, these cluster will be more widely spaced in rapidity and thus have a smaller average multiplicity. By cluster, we have in mind, for example, the $\Delta(1236)$ and ρ resonances which decay to πN and $\pi\pi$, respectively. A second factor which suppresses baryon production is baryon number conservation, which in multiperipheral models restricts the possible vertices from which they can emerge, whereas meson production is not so constrained. We will return to this point in Sec. IV.

In this paper we will study a highly simplified multiperipheral model of coupled pseudoscalar mesons and baryons in which the production mechanism is the exchange of meson and baryon Regge trajectories. The effects of the relative masses and baryon conservation are exploited, while in the interests of simplicity many other effects are neglected entirely. In particular, we will ignore the distinction between different mesons and baryons and in effect sum over their respective species. The model's free parameters will be adjusted to give the usual energy dependence of total cross sections, and this requirement alone constrains baryon multiplicities to be small. This depends only on properties of the kernel. We are unable to estimate the precise value due to ignorance with respect to off-shell baryon extrapolations (see Sec. III). With a variety of input parameters, the upper bound on the ratio of the total baryon to total meson multiplicity is 5-10%, not far from the probable asymptotic experimental value.[9]

There has been some recent interest in hybrid models[7] of multiparticle production in which individual events are regarded as either "diffractive" or "multiperipheral." The former class is associated with pomeron exchange and with large rapidity gaps in the

distribution of final particles. The multiperipheral events are attributed to, say, the exchange of secondary Regge trajectories or elementary pions in the production amplitude and associated with the absence of large rapidity gaps in the final state. Each of the two mechanisms is assumed to lead to constant or near-constant cross sections, and the multiperipheral component is taken to be factorizable and to provide the asymptotically increasing portion of the multiplicity. The model we are discussing here may be nicely interpreted as just this multiperipheral component.

II. FORMULATION OF THE MODEL

For motivation we first review a multi-Regge model studied earlier in a different context by Chew and Snider.[4] Consider a world of one species of hadron and suppose the forward absorptive part, $A(s)$, satisfies the integral equation

$$A(s) = K(s) + \int_1^s \frac{ds'}{s'} V(s/s') A(s') \tag{2}$$

depicted in Fig. 2. The inhomogeneous term is approximated by a single narrow resonance,

$$K(s) = g\, s_0\, \delta(s - s_0)$$

and the kernel is taken to be

$$V(s/s') = \gamma (s/s')^{2\alpha - 1}\, \theta(\log s/s' - w)$$

where α is the exchanged trajectory, and w is given approximately in Eq. (1). The need for the step function may be understood kinematically as follows. Label momenta as in Fig. 3, with the parametrization (to leading order at large s):

$$p_a = (s/2m, \underset{\sim}{0}, s/2m)$$

$$p_b = (m, \underset{\sim}{0}, 0)$$

$$q = (q_0, \underset{\sim}{q}_\perp, q_3)\ .$$

Then

$$k^2 = (p_a - q)^2 = \frac{s}{m}(q_3 - q_0) + t + m^2$$

where $t = q^2$, and

$$s' = (p_b + q)^2 \approx 2 q_0 m\ .$$

Solving for q_0 and eliminating q_3 via

$$q_3 \approx q_0 - \frac{t + q_\perp^2}{2 q_0}\ ,$$

we have

$$k^2 = s_0 \approx t + m^2 - s\, \frac{t + q_\perp^2}{s'}\ .$$

If the cluster mass s_0 becomes large, as it will in our application, this constraint requires $s/s' \approx s_0/(-t)$ and Eq. (1) has qualitatively this effect. In practice we will employ (1) but vary w somewhat.

The coupling constants γ and g differ for the following reason: in an exact multiperipheral equation, these would be the same but A, K, and V would depend on the external and internal masses and the second term would include an integral over the reggeon masses. We wish to replace this complication by an effective overall coefficient and an average trajectory. If the kernel were factorizable, such a replacement would follow automatically.[8]

Introducing a Mellin transform,

$$A(\lambda) = \int_1^\infty ds\, s^{-\lambda-1} A(s) \qquad (3a)$$

Eq. (2) is reduced to

$$A(\lambda) = g\, s_0^{-\lambda} + \gamma \frac{e^{-w(\lambda-2\alpha+1)}}{\lambda - 2\alpha + 1} A(\lambda) .$$

Redefining constants slightly, we write this in the form

$$A(\lambda) = K_0(\lambda) + K(\lambda)\, S(\lambda)\, A(\lambda) \qquad (4)$$

where $K_0 = g\, s_0^{-\lambda}$, $K(\lambda) = g\, e^{-w\lambda}$, and $S = f(\lambda - 2\alpha + 1)^{-1}$, with f as an effective off-shell coefficient. This equation and its generalization to coupled channels will be the basis of our arguments. The solution of (4) is

$$A(\lambda) = \frac{1}{1 - KS} K_0 = \frac{(\lambda - 2\alpha + 1) g s_0^{-\lambda}}{\lambda - 2\alpha + 1 - fge^{-w\lambda}} .$$

If w is given, the product fg is determined by requiring the solution to have a real pole at $\lambda = \lambda_0$, say, and then there is an assortment of complex secondary poles to the left. The inverse transform is

$$A(s) = \int_{c-i\infty}^{c+i\infty} \frac{d\lambda}{2\pi i} s^\lambda A(\lambda) \qquad (3b)$$

where Re(c) is to the right of all singularities of $A(\lambda)$. This gives

$$A(s) = s^{\lambda_0} a(\lambda_0) + \cdots$$

where a is the residue and the dots refer to nonleading contributions. Alternatively the transform can be carried out exactly by first expanding the denominator in $fge^{-w\lambda}$ (which amounts to solution by iteration of the kernel) to get

$$A(s) = K(s) + g\left(\frac{s}{s_0}\right)^{2\alpha-1} \sum_{n=1}^{\infty} \frac{(fg)^n}{(n-1)!} \left(\log\frac{s}{s_0} - nw\right)^{n-1} \cdot \theta\left(\log\frac{s}{s_0} - nw\right) .$$

From (4), each appearance of a factor g corresponds to the production of a single resonance, so the term proportional to g^n is the n-resonance intermediate state contribution to the absorptive part, which appears only when its "threshold" is reached. The various moments of the multiplicity distribution can now be calculated by

$$\langle n \rangle A(s) = g \frac{\partial}{\partial g} A(s) ,$$

$$\langle n(n-1) \rangle A(s) = g^2 \frac{\partial^2}{\partial g^2} A(s) ,$$

and so on.

Now for the remainder of the paper we imagine a world of pseudoscalar mesons and baryons and extend the above results to the coupled-channel case. For simplicity we will make no further distinctions among particles and our results should be interpreted as if we had summed over meson and baryon species. We have to consider MM, MB, BB, and $B\bar{B}$ absorptive parts, so in the t-channel, where the integral equations are diagonalized, MM, $B\bar{B}$, and $\bar{B}B$ channels are required. Our Mellin transformed integral equation is the same as (4) above, except that each entry is a 3×3 matrix. The kernel is

$$K(\lambda) = \begin{pmatrix} G_1 & G_3 & G_3 \\ G_3 & G_2 & 0 \\ G_3 & 0 & G_2 \end{pmatrix}$$

where the matrix elements refer to the t-channels $\pi\pi$, $B\bar{B}$, and $\bar{B}B$ respectively and $G_1 = g_i e^{-w_i\lambda}$, the w_i being the step parameters associated with the various resonances. The equalities between couplings follow from our neglect of charge and isospin distinctions and the two zero elements correspond to the neglect of exotic resonances of baryon number two. The inhomogeneous term K_0 has the same structure, but with G_i replaced by $g_i s_i^{-\lambda}$, s_i being the squared resonance mass. The reggeon propagator is

$$S(\lambda) = \begin{pmatrix} S_M(\lambda) & 0 & 0 \\ 0 & S_B(\lambda) & 0 \\ 0 & 0 & S_B(\lambda) \end{pmatrix}$$

where $S_{M,B} = f_{M,B}(\lambda - 2\alpha_{M,B} + 1)^{-1}$. The f's are the result of approximating the off-shell dependence as described above. It is known that off-shell extrapolations of baryons are anomalously large,[10] so f_M and f_B are likely to differ substantially from each other and from unity.

If we now perform a linear transformation to the channels MM, $\frac{1}{2}(B\bar{B} + \bar{B}B)$, and $\frac{1}{2}(B\bar{B} - \bar{B}B)$ and rescale g_2, the kernel becomes

$$K = \begin{pmatrix} G_1 & G_3 & 0 \\ G_3 & G_2 & 0 \\ 0 & 0 & G_2 \end{pmatrix} .$$

The inhomogeneous term has the same structure and S is unchanged. The third channel, $\frac{1}{2}(B\bar{B} - \bar{B}B)$ is thus decoupled from the others and has just the form of the single channel model discussed above. The resulting equations for the two coupled channels are depicted in Fig. 4, where the dashed and solid lines refer to mesons and baryons, respectively.

We will assume the MM cluster is a relatively low mass resonance such as the ρ, and simplify our labor slightly by neglecting its thresholds (i.e., set $w_1 = 0$). This should be harmless as these thresholds are only important at low energies and we are chiefly interested in baryon thresholds.

Suppressing the decoupled channel, the final forms of the various matrices are:

$$K_0(\lambda) = \begin{pmatrix} g_1 s_1^{-\lambda} & g_3 s_3^{-\lambda} \\ g_3 s_3^{-\lambda} & g_2 s_2^{-\lambda} \end{pmatrix} , \tag{5}$$

$$K(\lambda) = \begin{pmatrix} g_1 & g_3 e^{-w_3\lambda} \\ g_3 e^{-w_3\lambda} & g_2 e^{-w_2\lambda} \end{pmatrix} , \tag{6}$$

$$S(\lambda) = \begin{pmatrix} f_M(\lambda - 2\alpha_M + 1)^{-1} & 0 \\ 0 & f_B(\lambda - 2\alpha_B + 1)^{-1} \end{pmatrix} . \tag{7}$$

We will use $\alpha_M = 0.5$ for the meson trajectory. This may be regarded as either the exchange of the usual vector and tensor meson trajectories or as an effective pion trajectory in an ABFST-like model.[11] For the baryon trajectory we will vary α_B between 0, corresponding to an average intercept, and -1 to take into account the fact that $t_{min} \neq 0$ for the baryon reactions occurring along the multiperipheral chain.

III. SOLUTION

The matrix inversion of (4), together with (5), (6), and (7), gives

$$A(\lambda) = \frac{1}{D(\lambda)} \begin{pmatrix} N_{11}(\lambda) & N_{12}(\lambda) \\ N_{21}(\lambda) & N_{22}(\lambda) \end{pmatrix} \tag{8}$$

where the explicit forms of the N_{ij} will not be needed and the common denominator function is

$$\begin{aligned} D(\lambda) &\equiv f_M f_B (S_M S_B)^{-1} \det(1 - KS) \\ &= (\lambda - 2\alpha_M + 1 - g_1 f_M)(\lambda - 2\alpha_B + 1 - g_2 f_B\, e^{-w_2}) \\ &\qquad - f_M f_B\, g_3^2\, e^{-2w_3\lambda} . \end{aligned} \tag{9}$$

The third, decoupled channel has the solution

$$A_{33}(\lambda) = \frac{(\lambda - 2\alpha_B + 1) g_2 s_2^{-\lambda}}{\lambda - 2\alpha_B + 1 - f_B g_2\, e^{-w_3\lambda}} . \tag{10}$$

We would now like to determine as many of the coupling constants as possible. First, the total cross sections for the coupled channels should have constant and $s^{-\frac{1}{2}}$ terms corresponding to the P and P' trajectories, so we require $D(1) = D(\alpha_{P'}) = 0$ where $\alpha_{P'} \approx \frac{1}{2}$. At this point we can see that the effective off-diagonal coupling, $z \equiv f_M f_B (g_3 e^{-w_3})^2$, cannot be large. First note that the coupling constants must be real, since they are proportional to cross sections. From (9) and our two requirements, $D(\lambda)$ must have roughly the form shown in Fig. 5. If z is too large, the left part of the curve is pulled down by the exponential in λ in (9) (provided $w_3 > w_2$, which we will justify below) and the second zero will be absent. It will be shown that the baryon multiplicity is proportional to z and so is prevented from becoming large.

Unfortunately we have no reasonable method to fix all of the remaining parameters. The resonance masses and $|t_{max}|$ can be inferred accurately enough for our purposes from experiment, but this leaves three coupling constants and two off-shell parameters. We have two constraints on $D(\lambda)$ and could also use asymptotic cross section data, but by factorization there are only two independent total cross sections and so one free parameter remains. For reasons we will elaborate upon below, the model does not reliably treat the magnitudes of the contributions of secondary Regge poles. We could use data on multiplicities, but we are trying to calculate these. A last possibility would be to require the decoupled channel to have a pole at $\lambda \sim \frac{1}{2}$, corresponding to the ω trajectory. This requirement is untenable, because in the absence of the off-diagonal coupling the symmetric and antisymmetric $B\bar{B}$ channels alone generate exactly exchange degenerate P' and ω trajectories.[12] As the coupling to the MM channel increases from zero, the P' is perturbed away from the ω, so to insist on exchange degeneracy is to explicitly require z to be small. In a better model, of course this defect would be overcome by introducing additional coupling to the ω.

As we will show momentarily, the asymptotic average multiplicities depend only on the denominator function $D(\lambda)$ which we can

compute simply by varying z and then requiring $D(1) = D(\alpha_{P'}) = 0$. Thus, fortunately, the multiplicities will essentially depend only on the properties of the kernel. We could then adjust f_M and f_B so that the total cross sections agree with experiment, but there seems little point in so doing.

We now specify the resonance parameters further, taking as our guide the πN system. The low energy πN total cross section is dominated by the $\Delta(1236)$ and in addition there is likely to be a significant contribution from the nucleon pole below threshold.[13] If we take the average of the squared masses and assume that $|t_{max}|$ is effectively $\frac{1}{2}$ to 2 GeV^2, we obtain from Eq. (1) that $\cosh w_3$ is between 1.6 and 3.5. To be safe we will allow $\cosh w_3$ to vary over a still larger range, from 1.5 to 7.0. We next assume that the $B\bar{B}$ kernel is dominated by the same meson resonance as MM,[14] whose thresholds we have decided to suppress, and so $w_2 = 0$. While this is somewhat ad hoc, it is simple and not unreasonable. Notice that elastic $B\bar{B}$ scattering is present above threshold through coupling to MM.

The average multiplicities are given by

$$\langle n_B \rangle A(s) = z \frac{\partial}{\partial z} A(s)$$

$$\langle n_M \rangle A(s) = (2g_1 \frac{\partial}{\partial g_1} + 2g_2 \frac{\partial}{\partial g_2} + z \frac{\partial}{\partial z}) A(s) , \qquad (11)$$

where we have assumed the MM and MB resonances decay to M + M and M + B, respectively. On differentiating and inverting the Mellin transform these multiplicities come out to be (primes refer to derivatives with respect to λ)

$$\langle n_B \rangle = \left[-z \frac{\partial}{\partial z} D(\lambda)/D'(\lambda) \right]_{\lambda=1} \log s + \cdots$$

$$= 2 \frac{(2 - 2\alpha_M - g_1 f_M)(2 - 2\alpha_B - g_2 f_B)}{D'(1)} \log s + \cdots$$

$$\langle n_M \rangle = 2 \frac{(2 - 2\alpha_M)(2 - 2\alpha_B) - g_1 g_2 f_M f_B}{D'(1)} \log s + \cdots$$

where the omitted terms are constant or falling in s. We have plotted these results as a function of z in Figs. 6 and 7 for the various choices of parameters listed in Table I. In these fits $(g_1 f_M)$ varies between 0.5 and 1.0 and $(g_2 f_B)$ between 1.5 and 2.0. For values of z larger than those shown, there is no solution with real coupling constants. Besides the two real poles at $\lambda = 1$ and $\alpha_{P'}$, the next leading singularity is a third real pole at $\lambda \approx -2$. By making use of the condition $D(1) = 0$, we can write

$$\frac{\langle n_B \rangle}{\langle n_M \rangle} \sim \frac{z}{4(1 - \alpha_M)(1 - \alpha_B) - g_1 g_2 f_M f_B} \ ;$$

the denominator turns out to be roughly constant as z increases, so this ratio is approximately a linear function of z, and is at most 5 to 10%.

The total two-meson correlation,

$$f_M^{\ 2} = \langle n_M(n_M - 1) \rangle - \langle n_M \rangle^2$$

can be obtained similarly and turns out to be of the form $a \log s$ + constant, with a between 2.0 and 7.5. That this

quantity is positive follows from the fact that to the extent that the off-diagonal coupling is small, the mesons are being produced in pairs from a decaying resonance. The $\log^2 s$ term that might be present in f^2 is absent since this is a factorizable model. Experimentally f^2 is positive, and Harari and Rabinovici[7] have estimated in a fit to a hybrid model that f^2 of the multiperipheral component is an increasing function of $\log s$.

IV. DISCUSSION

First we note that the smallness of the baryon to meson ratio is essentially due to the structure of the model and the fact that the baryons are only produced at the off-diagonal vertex which is comparatively weak. The resonance and trajectory parameters have a small effect, mainly because they can be compensated by the coupling constants.

The obvious question to ask at this point is whether the small baryon multiplicity will be present in a more realistic model, and we feel the answer is yes. The essential ingredient, as we saw in Sec. III, was the shape of $D(\lambda)$ in Fig. 5. In a more realistic two-channel model, in the trace approximation for example, the fixed poles we have used are replaced by cuts and instead of a single narrow resonance there might be the Mellin transform of the low energy cross section. However, for large positive λ, $D(\lambda)$ will increase rapidly and for large negative λ it will still decrease exponentially to $-\infty$, provided the dominant mass is that associated with the MB kernel [this term enters $D(\lambda)$ with a negative sign]. In this case we expect $D(\lambda)$ to have essentially the same form as in Fig. 5, with more structure, especially around $\lambda = 0$ to 1. It will still be true that if the coupling to the (large) MB mass becomes too large, the left half of the curve will be drawn down and the secondary poles (zeros of D) will be absent. The particular values we obtained for the average multiplicities are a result of the procedure used for fixing the coupling constants, but this mechanism will be present in more realistic models. Thus we see that the essential ingredient in our argument is that the baryons be produced from $\alpha_M - B^* - \alpha_B$

vertices where the mass of B^* is the largest important mass in any of the kernels. In this more general context we are of course unable to give numbers, but in the special model we have treated the baryon multiplicity is small for a wide range of parameters and it seems likely that this effect will persist.

We place little reliance in the contribution of secondary Regge trajectories in the model mainly because we have used them as input to control the leading trajectory in the output, and it seems too much to ask that they give a reasonable secondary output as well. In fact it turns out that the model predicts that some total cross sections approach their limit from below, contrary to experiment. This problem is essentially the result of an oversimplified kernel.

In conclusion, we believe we have shown how the small production of baryons relative to mesons at high energy emerges naturally from a simple model embodying Regge behavior and multiperipheralism. While the particular crude model we have used is not adequate for understanding quantitative details, we feel the general features of the argument will be true in more realistic models.

ACKNOWLEDGMENTS

I thank Geoffrey F. Chew for suggesting this problem and for considerable advice and criticism, and Mordechai Bishari and Cristian Sorensen for helpful discussions.

FOOTNOTES AND REFERENCES

* This work was supported by the U. S. Atomic Energy Commission.

1. J. C. Sens, Oxford Conference Report (CERN preprint).

2. That the ratio will not increase further with energy is likely in view of Fig. 1.

3. D. Amati, A. Stanghellini, and S. Fubini, Nuovo Cimento 26, 896 (1962).

4. G. F. Chew and D. R. Snider, Phys. Letters 31B, 75 (1970).

5. C. F. Chan and B. R. Webber, Phys. Rev. D5, 933 (1972).

6. Amusingly, this effect can be obtained by dimensional analysis: since

$$\langle n_c \rangle = \frac{1}{\sigma_{ab}} \int dp_c \frac{d\sigma(ab \to cX)}{dp_c} ,$$

on dimensional grounds we might say $d\sigma(ab \to cX) \sim m_c^{-2}$, whence $\langle n_N \rangle / \langle n_\pi \rangle \sim (m_\pi/m_N)^2 \sim 2\%$. Similarly $\langle n_k \rangle / \langle n_\pi \rangle \sim 8\%$, which also roughly agrees with experiment.

7. K. Wilson, Cornell Report CLNS 131 (1970); K. Fialkowski, Phys. Letters 41B, 379 (1972); W. R. Frazer, R. D. Peccei, S. S. Pinsky, and C.-I Tan, La Jolla preprint UCSD-10P10-113; H. Harari and E. Rabinovici, Weizmann Institute Report.

8. G. F. Chew and W. R. Frazer, Phys. Rev. 181, 1914 (1969).

9. D. R. O. Morrison, Oxford Conference Report (CERN preprint D. Ph. II/PHYS 72-19).

10. See, for example, V. Barger and D. Cline, Phys. Rev. Letters 19, 1504 (1967).

11. G. F. Chew and D. R. Snider, Phys. Rev. D1, 3453 (1970); G. F. Chew, T. Rogers, and D. R. Snider, Phys. Rev D2, 765 (1970).

12. See in this connection P. D. Ting, Phys. Rev. 181, 1942 (1969).

13. C. F. Chan, Phys. Rev. D4, 3466 (1971).

14. For related work on $B\bar{B}$ annihilation in the multiperipheral model see H. Goldberg, Phys. Rev. D6, 2542 (1972).

Table I. Parameters for Figs. 6 and 7.

Curve number	cosh w_3	α_B	$\alpha_{P'}$
1	1.5	-0.5	0.5
2	7.0	-0.5	0.5
3	3.5	-1.0	0.5
4	3.5	0.0	0.5
5	3.5	-0.5	0.3
6	3.5	-0.5	0.7

FIGURE CAPTIONS

Fig. 1. $\bar{p}/\pi^-$ ratio at various energies.

Fig. 2. Schematic multiperipheral equation.

Fig. 3. Kinematics for Fig. 2.

Fig. 4. Coupled-channel multiperipheral equations.

Fig. 5. Form of the denominator function.

Fig. 6. Coefficient of log s in $\langle n_M \rangle$.

Fig. 7. Coefficient of log s in $\langle n_B \rangle$.

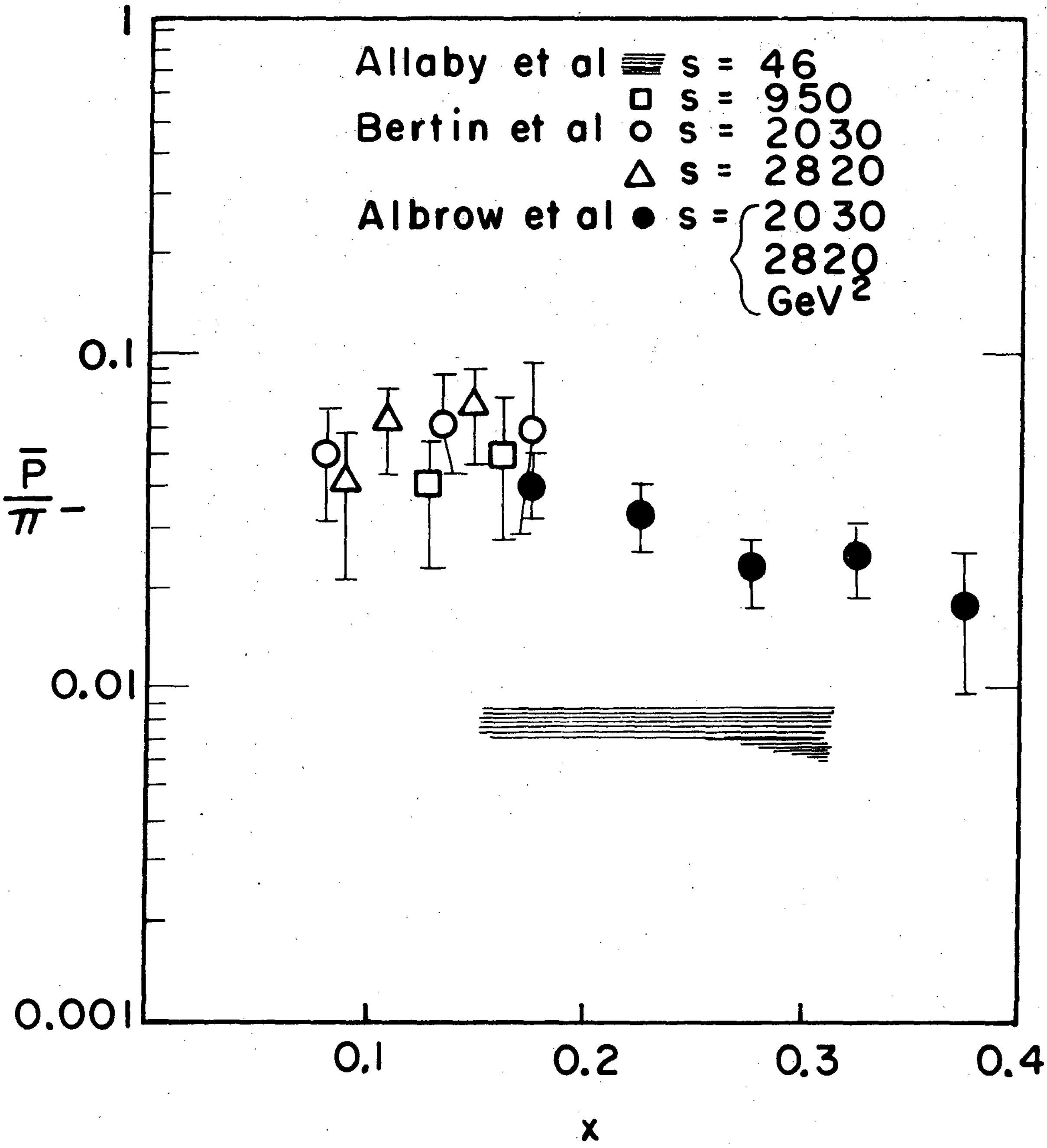

XBL7212-4971

Fig. 1

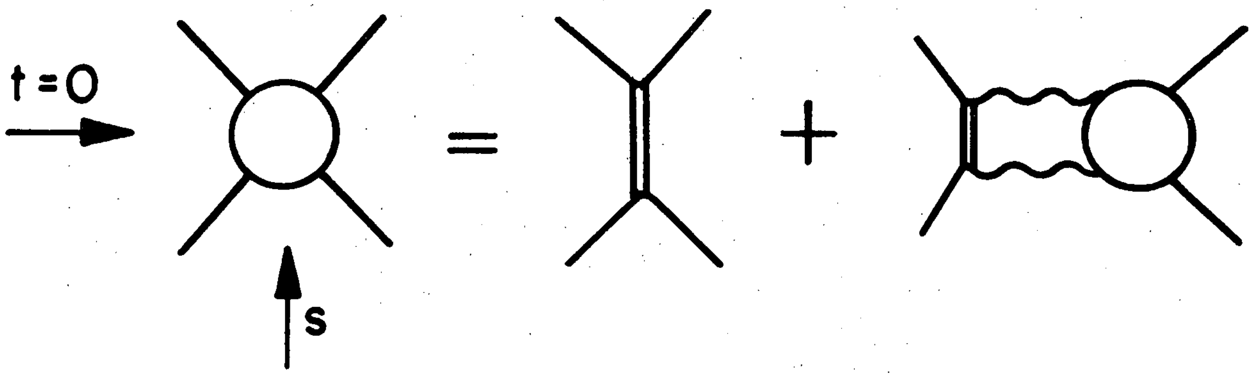

XBL7212 -4967

Fig. 2

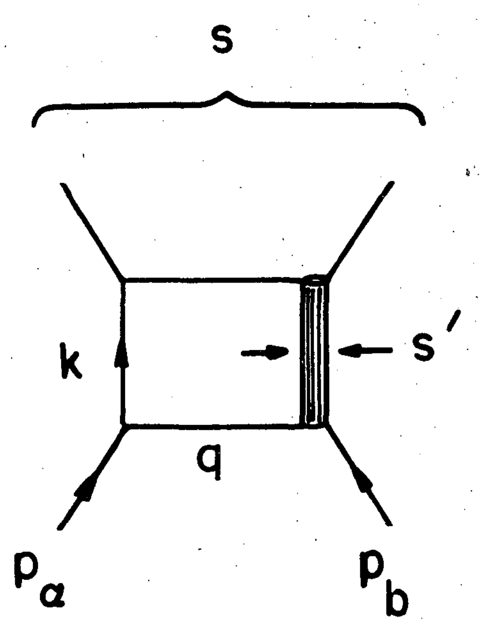

XBL7212-4969

Fig. 3

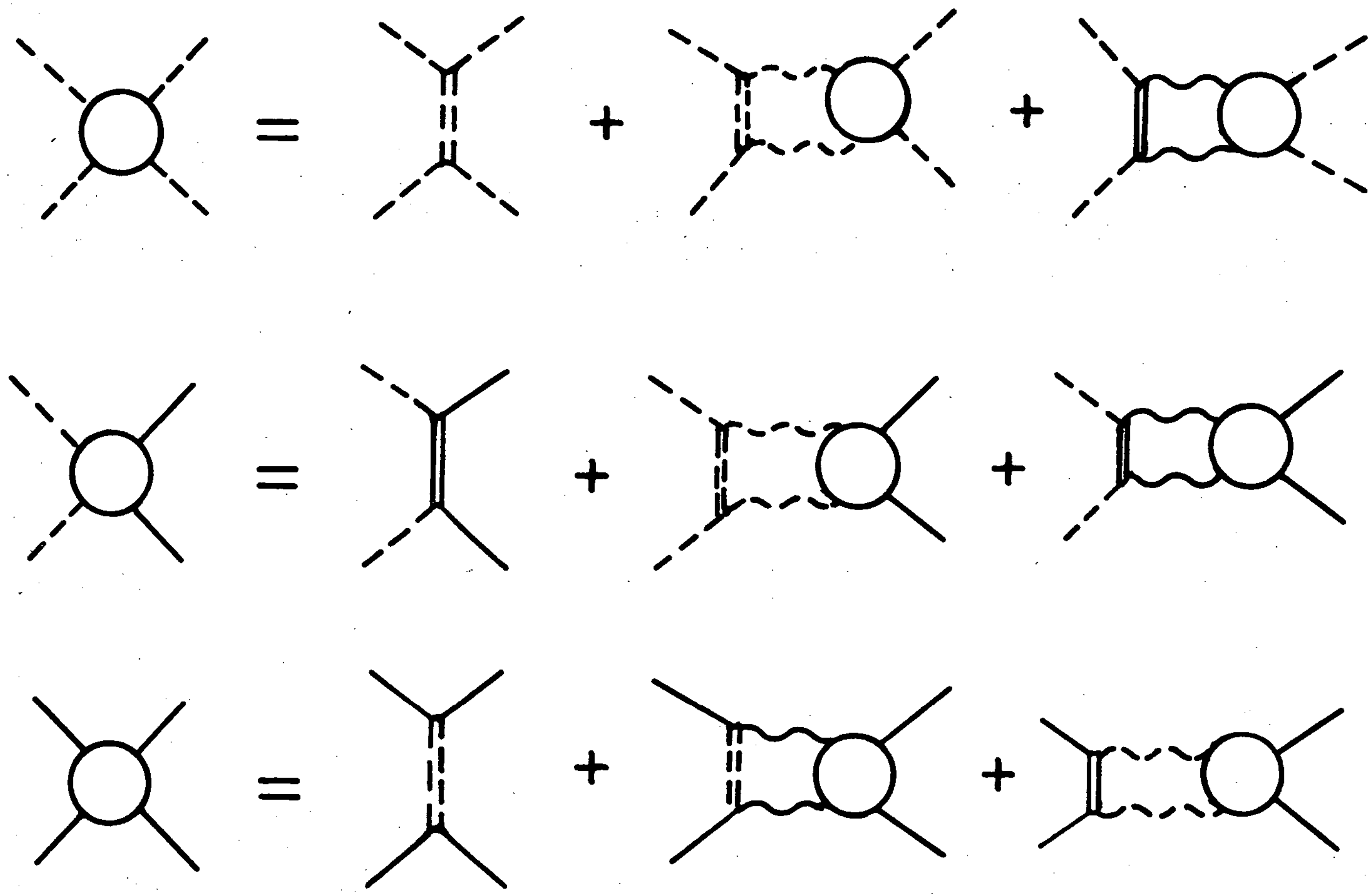

XBL7212-4970

Fig. 4

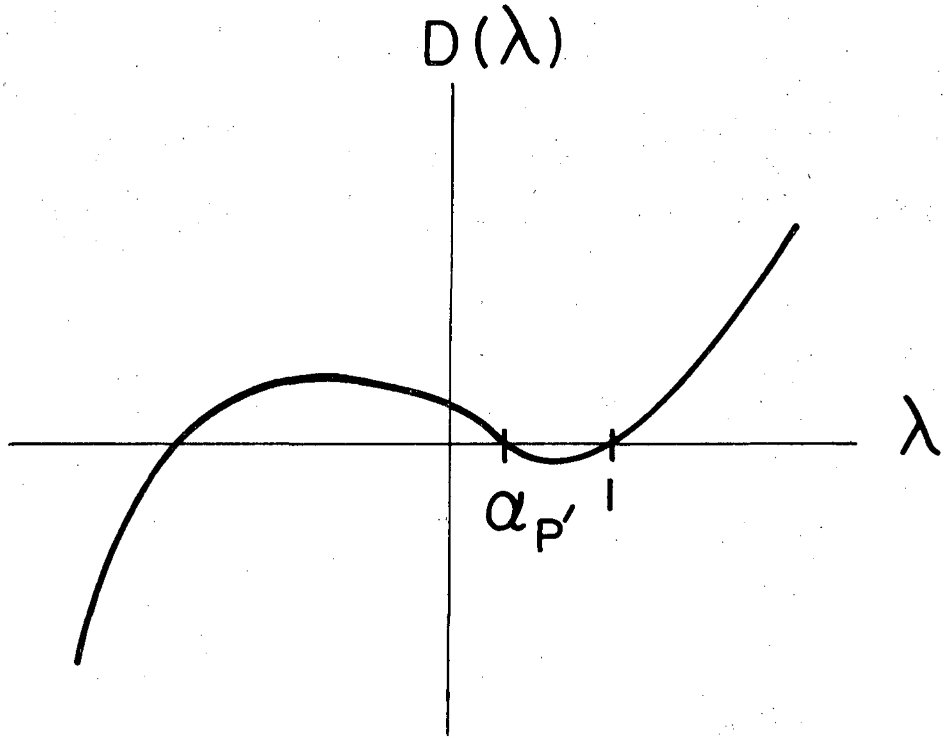

XBL7212-4968

Fig. 5

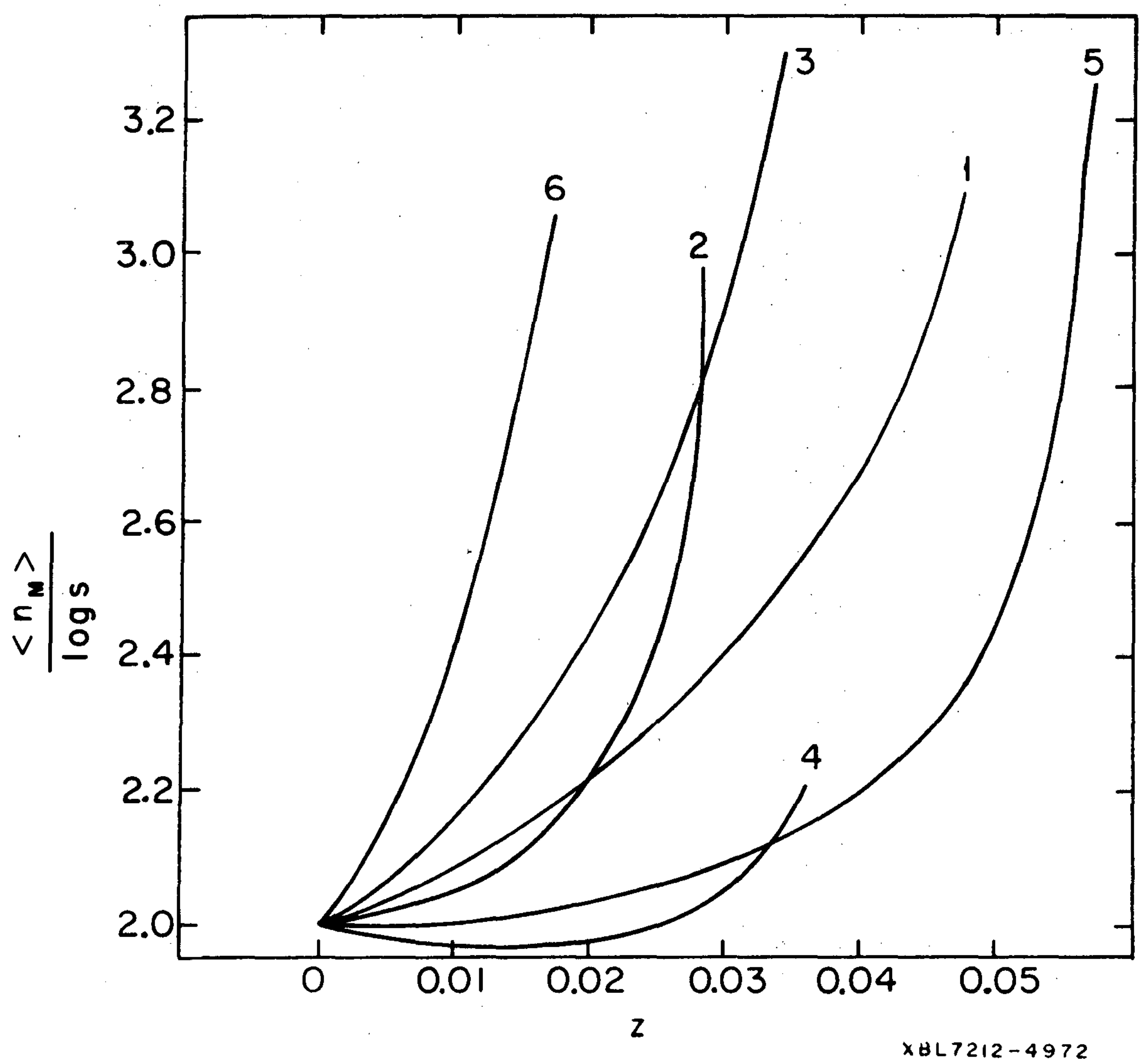

3.2
3.0
2.8
2.6
2.4
2.2
2.0
$\frac{\langle n_w \rangle}{\log s}$
0
0.01
0.02
0.03
0.04
0.05
z
1
2
3
4
5
6
XBL7212-4972

Fig. 6

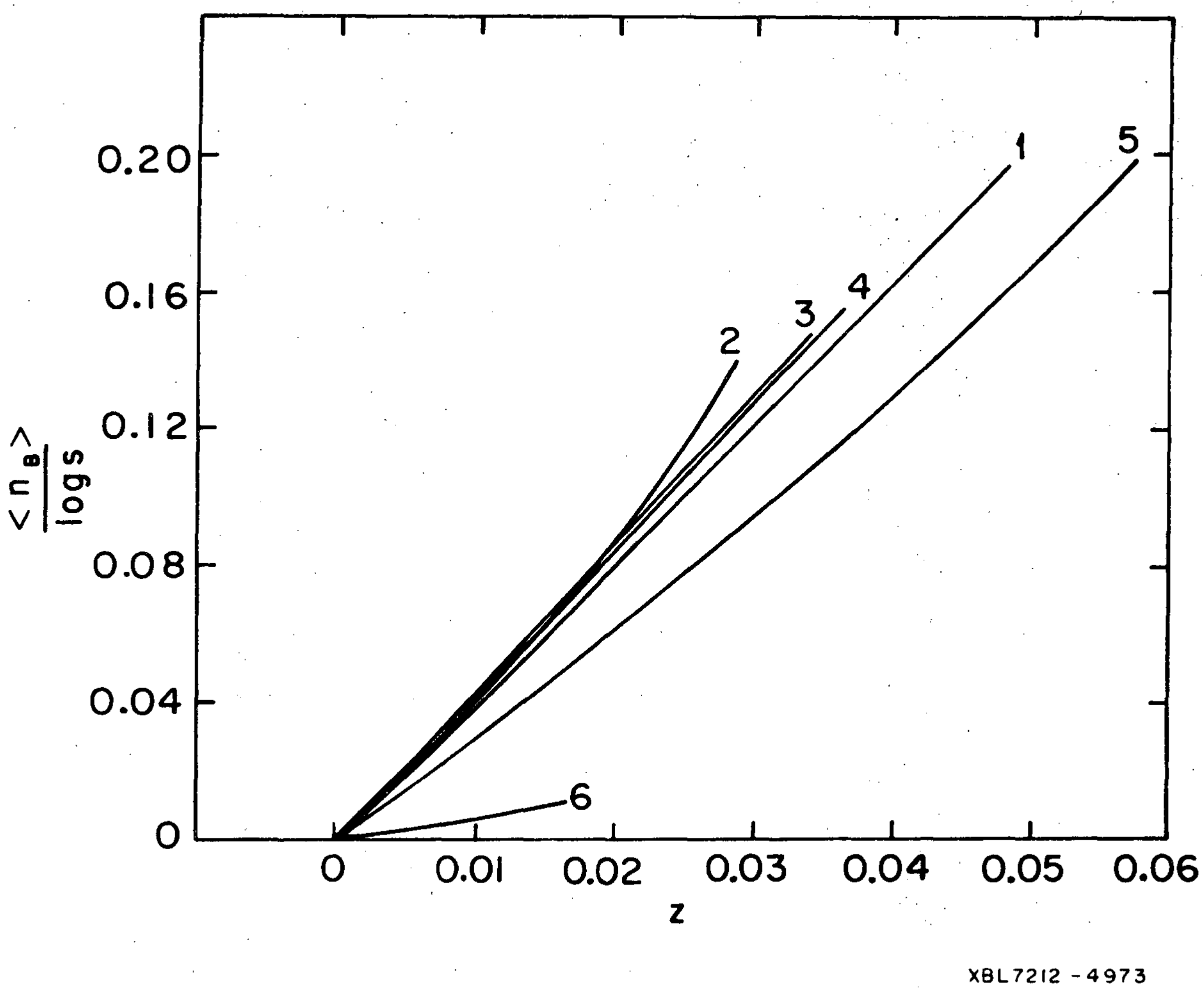
0.20
0.16
0.12
0.08
0.04
0
$\frac{<n_B>}{\log s}$
0
0.01
0.02
0.03
0.04
0.05
0.06
z
1
2
3
4
5
6
XBL7212 -4973

Fig. 7

TECHNICAL INFORMATION DIVISION
LAWRENCE BERKELEY LABORATORY
UNIVERSITY OF CALIFORNIA
BERKELEY, CALIFORNIA 94720